Near Term Improvements to WAAS Availability

Juan Blanch, Todd Walter, R. Eric Phelts, Per Enge

Stanford University

ABSTRACT

Since 2003, when it was first declared operational, the Wide Area Augmentation System (WAAS) has been increasing its availability through successive software updates (for example, new monitoring algorithms) and hardware updates (expanded reference receiver network). Today, WAAS provides vertical guidance to more than 3000 runways in the United States. With the current GPS constellation, WAAS has very high availability, and is even robust to some degradation in the constellation. However, even with the current GPS constellation, WAAS availability can be affected by the loss of a single satellite. In addition, there is growing interest in using WAAS for more demanding operations, such as Autoland. For these reasons, it is worthwhile investigating possible improvements in the ground monitors (which would not require avionics updates).

In this paper, we propose and evaluate changes in three areas of the monitoring algorithms: signal deformation monitoring, code noise and multipath characterization, and clock and ephemeris monitoring. We show that even without reducing the ionospheric delay error bounds, which are the biggest contributor to the Protection Levels, it is possible to significantly increase WAAS performance.

INTRODUCTION

The United States has operated the Wide Area Augmentation System (WAAS) in North America since 2003. WAAS improves the accuracy of GPS to the meter level, and mitigates the faults and space weather effects that affect the integrity of stand-alone GPS. With the use of ranging from the GEO satellites, it also reduces aviation's sensitivity to the strength of the GPS constellation. In the United States more than 70,000 aircraft are currently equipped with suitable avionics, and approximately 3000 runways across the United States have LPV approach procedures based on WAAS (twice as many as there are Instrument Landing System glide slopes) [1]. In addition, WAAS has enabled the development of many missed approach procedures, and departure guidance for numerous runway ends and heliport/helipads in the National Airspace System [2].

As users become increasingly reliant on the performance and capabilities of single frequency WAAS, it will be necessary to maintain or even increase its level of service. In particular, WAAS should be robust to changes in the GPS constellation. Although it is not possible to make WAAS insensitive to any change in the constellation, it might be possible to increase its robustness, especially at the edge of coverage. In this paper, we investigate changes in the integrity monitoring algorithms [3]. Although changes in the monitoring algorithms can be costly, they do not require hardware updates; and, more importantly, they do not require modifications at the user receiver level. Specifically, we propose and evaluate changes in three areas: code noise and multipath processing [4], signal deformation monitoring [5], and the clock and ephemeris integrity algorithm.

OVERVIEW OF INTEGRITY MONITORS

Figure 1 shows a high level overview of the major integrity monitors. Code Noise and Multipath (CNMP) algorithms process the receiver measurements from each of three receivers at 38 reference stations. Inconsistent measurements are identified and removed or deweighted, and then used for carrier smoothing. The residual multipath and noise effects are bounded by the CNMP curve. These cross checked and smoothed measurements are passed on to the other monitors.

Threats are grouped into one of two categories: those that are likely to affect only a single satellite's ranging accuracy, or those that affect the ionospheric estimation at each grid point. The first set of threats is protected by the broadcast UDRE for each satellite and the second group is protected by the broadcast GIVE for each grid point. The UDRE is initially set by the monitor that evaluates the risk of clock and ephemeris threats for each satellite in view.

The Code Carrier Coherency monitor then evaluates if it can support that same UDRE or if it needs to be increased. Next, the Signal Quality Monitor evaluates if it can support the UDRE resulting from the previous two monitors.

Because the clock and ephemeris threat creates errors that may be spatially varying, it generally has greater uncertainty than other satellite threats for the L1-only user. Most often it is the monitor that determines the minimum UDRE that can be safely broadcast. The UDRE is combined by a shaping matrix broadcast in Message Type 28 [6]. This matrix accounts for the spatial variation of the clock and ephemeris error bound.

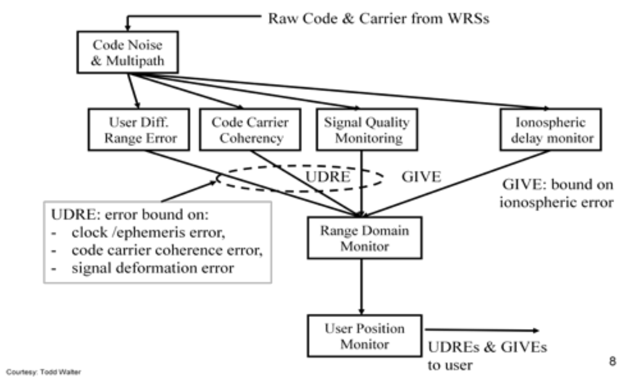

Figure 1. Overview of major integrity monitors

In parallel, the GIVE monitor determines the ionospheric corrections and the confidence bound that must be applied to each. These ionospheric terms are then combined with the satellite corrections and the UDREs to determine if the total L1 correction on each line of sight between the reference stations and the satellites are properly bounded by the UDRE and GIVE terms. This comparison is made by the Range Domain Monitor (RDM) which ensures that the individual corrections can be combined. The primary threat addressed by this monitor is related to interfrequency biases.

Finally, all of the corrections applied to each reference station result in a net WAAS positioning error that is checked against the known survey coordinates of the reference receiver's antenna. This error is compared to a much reduced version of the broadcast bound to ensure that smaller errors, that may not trip the previous monitors, will not combine in a way to create large position errors. This test is performed by the User Position Monitor (UPM. If either the RDM or UPM observe faults or lack the observability to validate the input UDREs and GIVEs, they will be increased or flagged unsafe by these monitors.

BASELINE PERFORMANCE

We will assess WAAS performance using the MATLAB Availability Simulation Tool (MAAST) [7], a service volume model tool that computes the Protection Levels (PLs) that would be experienced by WAAS users. MAAST simulates the WAAS message (GIVE, UDRE, and MT 28, without accounting for events that deviate from nominal behavior), determines the geometries experienced by users, computes the corresponding pseudorange error models, and calculates the PLs.

For all simulations, we used the GPS almanac corresponding to August 28th, 2012. Protection Levels were computed for a one by one degree grid of users over North America for a period of 24 h every 300 s. Figure 2 shows the 99% quantile of the VPL at every location as computed by MAAST, configured to simulate current WAAS performance. It can be seen that there is very good coverage of 35 m VPL (necessary for LPV-200).

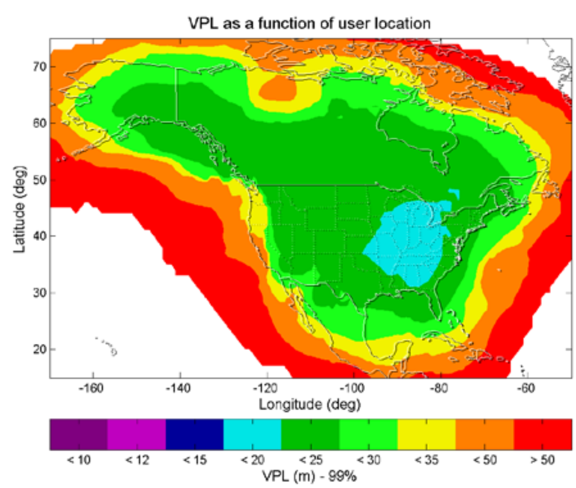

Figure 2. Map of the 99% quantile of the VPL for the baseline case.

BASELINE PERFORMANCE WITH DEGRADED CONSTELLATION

In this section we show what can happen to performance when as little as one satellite is unavailable. Again, we use the almanac corresponding to August 28th, 2012, but we remove PRN 21. This satellite was chosen because it actually was out for maintenance between August 28th and August 29th, 2012 [8]. This outage had a significant impact on coverage, as shown in Figure 3 (extracted from [8]). A drop in coverage from 97% to below 80% can be observed on August 29th.

In Figure 4, we show the simulated performance corresponding to this degraded constellation (the simulated performance is worse than the actual performance, because PRN 21 was not out during all 24 h).

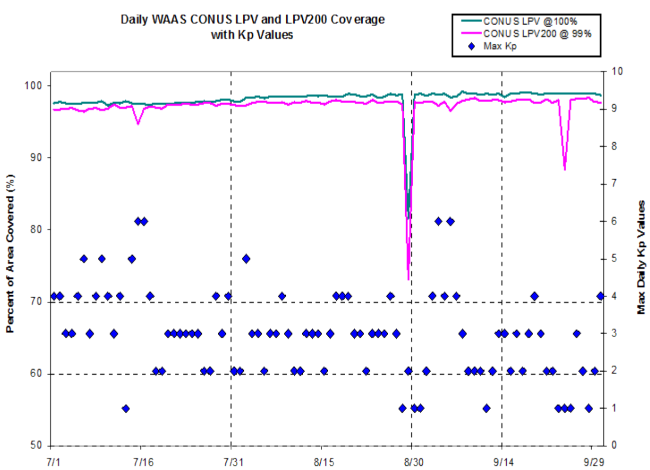

Figure 3. Coverage as a function of time for CONUS. The dip on August 29th, 2013 is due to the PRN 21 outage (Courtesy of the FAA).

In the next sections, we will take the conditions illustrated in Figure 4 (PRN 21 out) and evaluate the effect of changes in the monitoring algorithms.

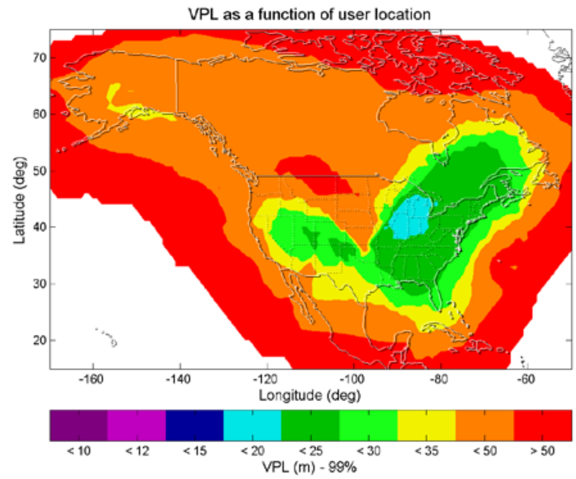

Figure 4. Map of the 99% quantile of the VPL for the baseline case with PRN 21 out

CHANGES IN THE LOWER MINIMA IMPOSED BY SIGNAL DEFORMATION MONITORING

Within the next two years (2014-2015), reference receivers in the ground monitoring network will be replaced by new receivers with enhanced capabilities [9]. The new receivers will have a larger bandwidth and improved signal deformation measurements [9]. The improved receiver performance combined with a new design of the signal deformation monitor could result in a better detection of signal deformation. As described above, the effect of the signal deformation monitor is to impose a minimum value for both the GIVE and the UDRE. Currently, these minimum values are set to:

$$\sigma_{UDRE} = 0.91 \text{ m (UDREI 5)}$$

$$\sigma_{GIVE} = 0.91 \text{ m (GIVEI 9)}$$

With the new receivers and the improved monitors, the following minima appear to be feasible [9]:

$$\sigma_{UDRE} = 0.38 \text{ m (UDREI 2)}$$

$$\sigma_{GIVE} = 0.54 \text{ m (GIVEI 5)}$$

Figure 5 shows the WAAS performance under the conditions of Figure 4 with the new minima. Although the improvement is modest, it is not insignificant.

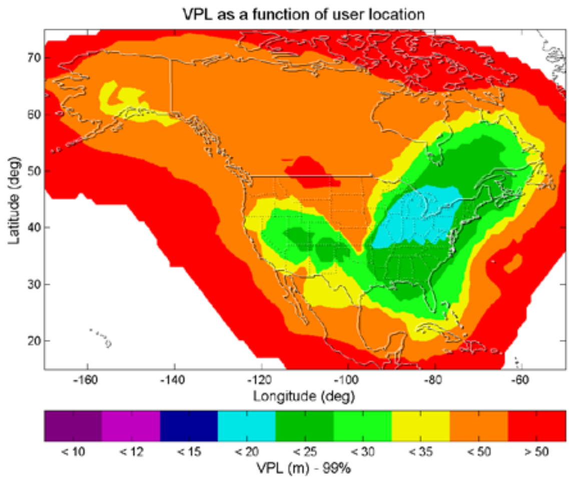

Figure 5. Map of the 99% quantile of the VPL for the baseline case with PRN 21 out and new minima for the UDRE and the GIVE

IMPROVEMENTS IN THE CODE NOISE AND MULTIPATH CURVE

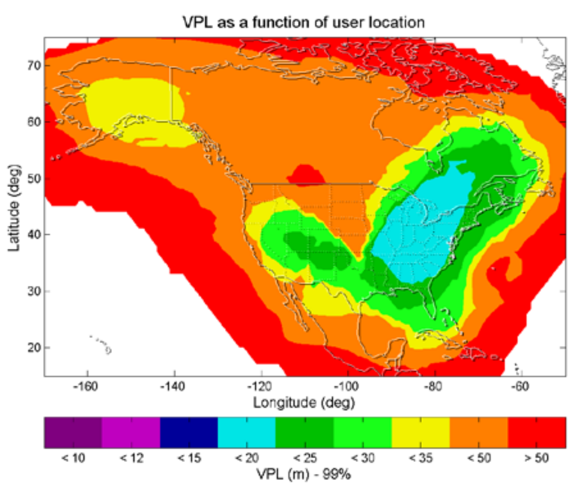

Figure 6. Map of the 99% quantile of the VPL for the baseline case with PRN 21 out, new minima for the UDRE and the GIVE, and a reduced CNMP curve

The code noise and multipath [4] is the error that affects the pseudorange measurements at the reference stations. This error affects the performance of all the integrity monitors. In WAAS, each reference station has three receivers which have, in most cases, a physical separation sufficient to ensure that the multipath affecting each of them is uncorrelated. Although this spatial diversity is exploited in the integrity algorithms, it is currently not used to reduce the nominal error affecting each reference station. In this section, we simply assume that the three threads are averaged before being used by the downstream monitors (see Figure 1). This could lead to a reduction of as much as $\sqrt{3}$. It should be noted that there might be other ways of reducing the CNMP curve (for example, by being less conservative in the error bounds).

The result of dividing the CNMP curve by $\sqrt{3}$ in addition to the lower minima of the previous section is shown in Figure 6. The improvement with respect to the baseline shown in Figure 4 is now much more apparent.

IMPROVEMENTS IN THE CLOCK AND EPHEMERIS ALGORITHM

In this section, we evaluate the potential benefits of a new clock and ephemeris integrity algorithm. This algorithm was proposed in the context of dual frequency WAAS in [10]. Here, we apply it to single frequency WAAS (to both GPS and GEO satellites). The most important feature of the new algorithm is the combination of the UDRE monitor and the Message Type 28 (MT28) shaping matrix [6] into a single monitor. As with the current algorithm, it is designed to protect against the difference between the satellite position assumed by the user receiver and the position estimated by the integrity monitor, nominal biases at reference stations, and undetected pseudorange errors at reference stations. The key to the feasibility of this algorithm is an efficient way of computing an overbound of a set of covariance matrices, including the UDRE minimum.

Figure 7 illustrates in a one dimensional diagram how the algorithm determines the UDRE and MT 28. Omitting the details, the algorithm computes the covariance for the estimation error for each configuration with one station out. This is done to account for the possibility of an undetected fault in one of the stations. There are as many covariance matrices as there are stations. The algorithm then computes a covariance $Cov_{overbound}$ that is above all of them, and is above the minimum allowed UDRE value (see Figure 7). The covariance $Cov_{overbound}$ is then sent as a σ^2_{UDRE} (the smallest projection of the covariance thus obtained) and the shaping matrix MT 28, obtained by normalizing the covariance $Cov_{overbound}$ by σ^2_{UDRE}. The discretization of the shaping matrix can be identical to the one performed in the current MT 28. More details on the specifics of the algorithm can be found in [10].

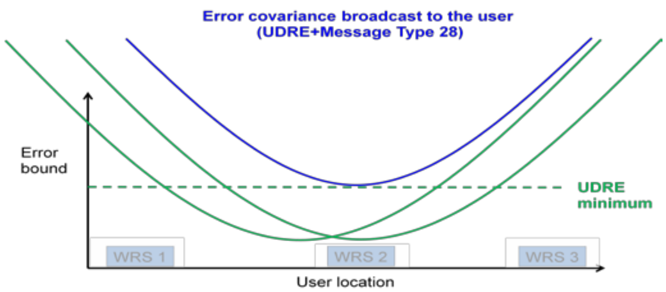

Figure 7. Diagram illustrating the generation of the UDRE and the shaping matrix MT 28

Figure 8 shows a histogram of the ratio between the user error bound corresponding to the clock and ephemeris error as computed with the proposed algorithm and the current one. There is the potential to reduce this contribution by more than 40%. For this reason, even if it is not the largest contributor to the total pseudorange error bound, it is worthwhile evaluating its potential.

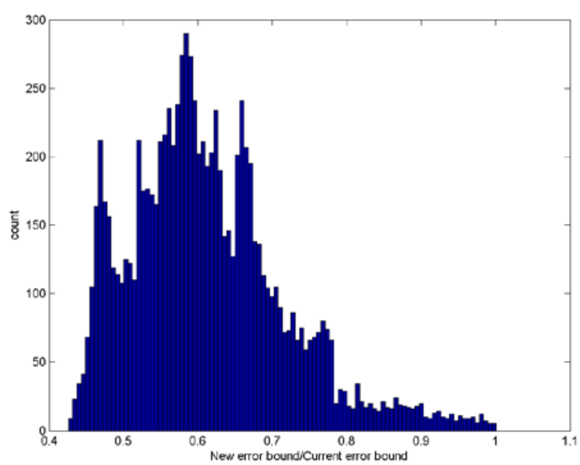

Figure 8. Histogram of New Clock and Ephemeris Error Bound/ Current Error Bound

This is confirmed by Figure 9, which shows WAAS performance with the proposed clock and ephemeris algorithm (in addition to the changes explained in the previous two sections). Almost all of CONUS and Alaska has 99% availability of LPV 200 (VPL<35 m), which is not the case in the baseline case shown in Figure 4.

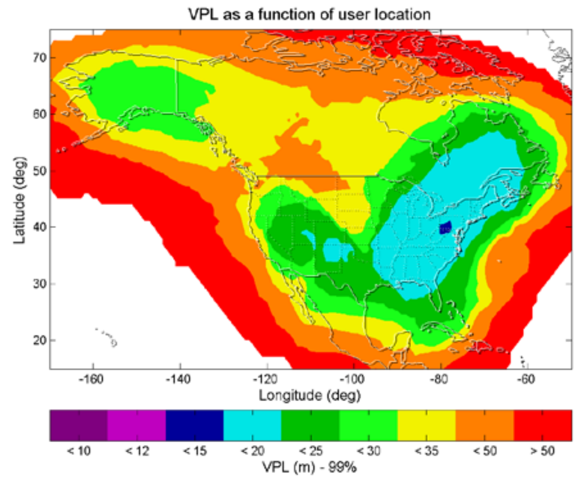

Figure 9. Map of the 99% quantile of the VPL for the baseline case with PRN 21 out, new minima for the UDRE and the GIVE, a reduced CNMP curve, and the proposed clock and ephemeris monitoring algorithm

Because of the significant improvement achieved with the addition of the new clock and ephemeris algorithm, we also evaluated the effect of changing only the clock and ephemeris algorithm (leaving the UDRE and GIVE minima and CNMP curve unchanged). The resulting VPL map is shown in Figure 10.

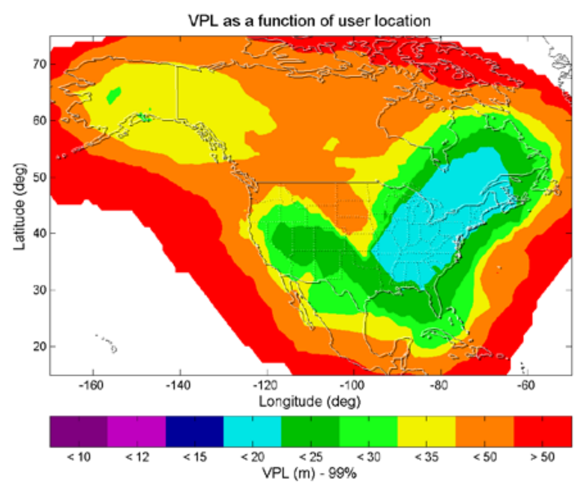

Figure 10. Map of the 99% quantile of the VPL for the baseline case with PRN 21 out, and the proposed clock and ephemeris monitoring algorithm

In Figure 11 we show the result of the proposed improvements to the full constellation, and should be compared to Figure 2. It can be seen that there are significant improvements in the *VPL*.

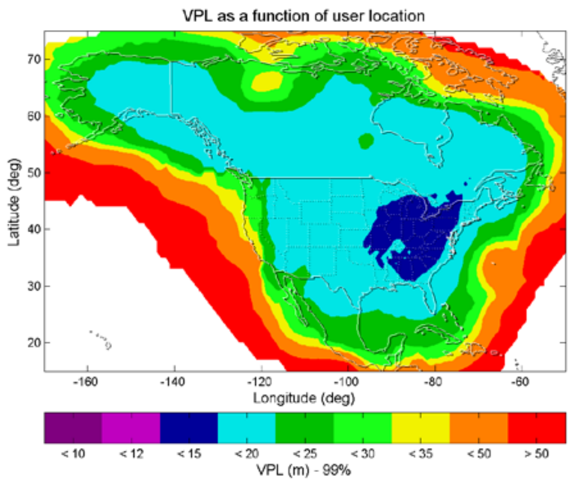

Figure 11. Map of the 99% quantile of the VPL for the baseline case, new minima for the UDRE and the GIVE, a reduced CNMP curve, and the proposed clock and ephemeris monitoring algorithm

CONCLUSION

This paper has evaluated the potential of changes in three areas of the WAAS monitoring algorithms: lowering the minimum GIVE and UDRE (by exploiting the new reference receivers and new signal deformation metrics), lowering the Code Noise and Multipath curve (for example by combining the three threads in each reference station, but other improvements are being considered), and applying a new clock and ephemeris algorithm (which combines the UDRE monitor and MT28).

The changes proposed here could greatly mitigate the effect of a degraded constellation, as well as improve the Protection Levels under nominal conditions, thus potentially facilitating new capabilities. These improvements would not require new avionics.

We also note that these improvements are obtained without changing the ionospheric error bound, which means that an even greater improvement could be expected in dual frequency WAAS.

ACKNOWLEDGEMENTS

This work was sponsored by the FAA GPS Satellite Product Team (AND-730).

REFERENCES

[1] http://www.faa.gov/about/office_org/headquarters_offices/ato/service_units/techops/navservices/gnss/approaches/index.cfm

[2] http://www.faa.gov/about/office_org/headquarters_offices/ato/service_units/techops/navservices/gnss/waas/news/

[3] Walter, T., Enge, P., and DeCleene, B., "Integrity Lessons from the WAAS Integrity Performance Panel (WIPP)," *Proceedings of the 2003 National Technical Meeting of The Institute of Navigation*, Anaheim, CA, January 2003, pp. 183-194.

[4] Shallberg, K. and Sheng, F., "WAAS Measurement Processing; Current Design and Potential Improvements," *Proceedings of IEEE/ION PLANS 2008*, Monterey, CA, May 2008, pp. 253-262.

[5] Phelts, R.E., Walter, T., Enge, P., "Characterizing Nominal Analog Signal Deformation on GNSS Signals," *Proceedings of the 22nd International Technical Meeting of The Satellite Division of the Institute of Navigation* (ION GNSS 2009), Savannah, GA, September 2009, pp. 1343-1350.

[6] Walter, Todd, Hansen, Andrew, Enge, Per, "Message Type 28," *Proceedings of the 2001 National Technical Meeting of The Institute of Navigation*, Long Beach, CA, January 2001, pp. 522-532.

[7] Jan, Shau-Shiun, Chan, Wyant, Walter, Todd, Enge, Per, "Matlab Simulation Toolset for SBAS Availability Analysis," *Proceedings of the 14th International Technical Meeting of the Satellite Division of The Institute of Navigation (ION GPS 2001)*, Salt Lake City, UT, September 2001, pp. 2366-2375.

[8] Wide-Area Augmentation System Performance Analysis Report #42. Available at: http://www.nstb.tc.faa.gov/

[9] Phelts, R.E., Walter, T., Enge, P., "Signal Deformation Monitoring for Dual-Frequency WAAS," *Proceedings of the 2013 International Technical Meeting of The Institute of Navigation*, San Diego, CA, January 2013

[10] Blanch, J., Walter, T., and Enge, P., "A Clock and Ephemeris Algorithm for Dual-Frequency SBAS," *Proceedings of the Institute of Navigation GNSS-11*, Portland, September 2011.